

Resonant pairing isotope effect in polaronic systems

Julius Ranninger¹ and Alfonso Romano²

¹*Centre de Recherches sur les Très Basses Températures,
Laboratoire Associé à l'Université Joseph Fourier,*

Centre National de la Recherche Scientifique, BP 166, 38042, Grenoble Cédex 9, France

²*Dipartimento di Fisica "E.R. Caianiello", Università di Salerno,
I-84081 Baronissi (Salerno), Italy - Unità I.N.F.M. di Salerno*

(Dated: November 6, 2018)

The intermediate coupling regime in polaronic systems, situated between the adiabatic and the anti-adiabatic limit, is characterized by resonant pairing between quasi-free electrons which is induced by an exchange interaction with localized bipolarons. The onset of this resonant pairing takes place below a characteristic temperature T^* and is manifest in the opening of a pseudogap in the density of states of the electrons. The variation of T^* is examined here as a function of (i) the typical frequency ω_0 of the local lattice modes, which determines the binding energy of the bipolarons, and (ii) the total concentration of charge carriers $n_{tot} = n_F + n_B$, where n_F and n_B are the densities of free electrons and bipolarons, respectively. The variation of either of these quantities induces similar changes of the value of n_B with respect to that of n_F , in this way leading to a shift of T^* . For finite, but small values of n_B (≤ 0.1 per site), we find negative and practically doping independent values of the corresponding isotope coefficient α^* . Upon decreasing n_{tot} such that n_B becomes exponentially small, we find a rapid change in sign of α^* . This is related to the fact that the system approaches a state which is more BCS-like, where electron pairing occurs via virtual excitations into bipolaronic states and where T^* coincides with the onset of superconductivity.

PACS numbers: PACS numbers: 74.20.Mn, 74.25.-q, 74.25.Kc

I. INTRODUCTION

The experimental verification of an isotope effect in the classical low temperature superconductors has been an unequivocal proof for phonon mediated electron pairing in form of Cooper pairs. Such a clearcut proof is so far absent in the high temperature superconducting cuprates (HTSC). Moreover, their proximity in the underdoped regime to an antiferromagnetic insulating state has largely contributed to conclude that in those materials pairing is associated with strong correlations. Nevertheless, the question concerning the origin of the pairing is far from being settled and lattice driven pairing ought not to be ruled out at this stage of our understanding. Actually, there is a certain amount of experimental evidence that strong electron-lattice coupling plays some role in stabilizing the superconducting phase in the cuprates. What is clear is that the pairing is definitely not of the form of a phonon mediated BCS one, corresponding to a weak coupling adiabatic regime.

Early on, anomalous mid-infrared optical absorption was found in virtually everyone of the superconducting cuprates. In lanthanum based compounds the superconducting critical temperature T_c was found to scale with the oscillator strength of this absorption^{1,2} and later on was shown to be due to polaronic charge carriers³. More refined measurements followed. From neutron scattering studies it became clear that the manifestation of the superconducting state in the cuprates could be intimately linked to strong electron-lattice coupling. A detailed analysis of the phonon density of states showed that the high-frequency modes are significantly renor-

malized in the superconducting materials as compared to their insulating parent compounds⁴. A further manifestation of strong electron-lattice coupling comes from the observation of a kink in the electron quasi-particle dispersion in the 50-80 mev energy region seen in angle resolved photo emission spectroscopy⁵. Finally, inelastic neutron scattering experiments pointed to an anomalous behavior in the dispersion of the in-plane longitudinal optical phonons with wave vectors [0, 0.25, 0] in the YBCO superconductors. This corresponds to bond stretching vibrations being associated with dynamical charge fluctuations on the Cu ions driven by the displacement of the neighboring ligand environment of the O atoms⁶.

Let us suppose, as a working hypothesis, that superconductivity in the cuprates is indeed controlled by strong electron-lattice coupling. If we want to test this assumption by examining the isotope effect in those materials, the right quantity to look at is not the transition temperature T_c , but the onset temperature of the electron pairing, T^* . T^* shows up in a qualitative change of the photoemission spectrum such that the electronic density of states exhibits a charge pseudogap as the temperature is decreased below T^* , eventually merging into a true superconducting gap below T_c . Pair formation in BCS superconductors coincides with the onset of a global phase-coherent superfluid state and hence the isotope effect can be evaluated on the basis of the shift in T_c . This does not apply to the HTSC, where it is a pair resonance state which sets in below T^* , implying pairing on a finite length and time scale. Only when this length and time scale gets longer and longer upon decreasing the temperature, a global phase-coherent state can be established, which is controlled by the center of mass motion

of the Cooper pairs rather than by their breaking up into individual electron pairs, as in the case of BCS superconductors. Considering that electron pairing is of resonance type rather than of a true bound electron pair nature, the different experimental setups devised to capture such a feature must rely on a time scale short enough to see this pairing as static. Thus, NMR or NQR cannot detect it since the relevant time scale has to be well below 10^{-8} sec. On the contrary neutron spectroscopy, studying the relaxation rate of the crystal field excitations, and X-ray absorption near edge spectroscopy (XANES) are in the right time scale regime of $[10^{-13}, 10^{-15}]$. And in fact it is those measurements on $\text{La}_{2-x}\text{Sr}_x\text{CuO}_4$ ^{7,10}, $\text{HoBa}_2\text{Cu}_4\text{O}_8$ ⁸ and $\text{La}_{1.81}\text{Ho}_{0.04}\text{Sr}_{0.15}\text{CuO}_4$ ⁹ which initially demonstrated this resonant pairing isotope effect.

We shall in this paper explore the resonant pairing isotope effect on the basis of a phenomenological model, believed to capture the intermediate coupling regime in polaronic systems, situated between the standard weak coupling adiabatic Born-Oppenheimer regime (applicable to BCS superconductors) and the anti-adiabatic regime, where the electrons pair up into bipolarons, expected to be localized at low temperatures. We have previously introduced such a model to study the connection between local dynamical lattice deformations, measurable by EX-AFS pair distribution functions¹¹, and the incoherent background expected in photoemission spectra, as interpreted in terms of phonon shake-off processes¹². On the basis of this model we shall show that the isotope effect of T^* can be traced back to the pairing energy of the bipolarons which is a linear function of the characteristic frequency of the local lattice modes.

In section II we briefly sketch this model and present a scheme to determine the doping and frequency dependence of T^* . Section III is devoted to a discussion of the results on the isotope coefficient and an attempt is made to relate its behavior to the isotope shift of the bipolaron binding energy and to the renormalization of the exchange coupling between the localized bipolaron and itinerant electrons. In the Conclusions, section IV, we make a comparison of these results with what is known presently from the experiments and suggest new ways of looking at this problem.

II. THE MODEL AND RESONATING PAIRING TEMPERATURE

Exact diagonalization studies¹³ in the crossover regime between the adiabatic weak coupling limit and the anti-adiabatic limit have led us to the conjecture that in this regime we are facing strong fluctuations between tightly bound pairs and uncorrelated pairs of free electrons, a scenario which can be phrased into a boson-fermion model. In order to incorporate into this model the information concerning the origin of the tightly bound electron pairs, we assume explicitly that they are of bipolaronic nature. The minimum model which can describe

such a situation is then given by the Hamiltonian

$$H = (D - \mu) \sum_{i,\sigma} n_{i\sigma} - t \sum_{\langle i \neq j \rangle, \sigma} c_{i\sigma}^+ c_{j\sigma}^- + (\Delta_B - 2\mu) \sum_i \left(\rho_i^z + \frac{1}{2} \right) + v \sum_i [\rho_i^+ c_{i\downarrow}^- c_{i\uparrow}^+ + \rho_i^- c_{i\uparrow}^+ c_{i\downarrow}^+] - \hbar\omega_0 \alpha \sum_i \left(\rho_i^z + \frac{1}{2} \right) (a_i + a_i^+) + \hbar\omega_0 \sum_i \left(a_i^+ a_i + \frac{1}{2} \right). \quad (1)$$

Here ρ_i^\pm denote the creation and annihilation operators for the electron pairs which, due to their interaction with the local lattice deformations $X_i = (a_i + a_i^+)/\sqrt{2M\omega_0/\hbar}$, end up in self-trapped bipolarons $\rho_i^\pm \exp[\pm\alpha(a_i - a_i^+)]$ localized on some effective sites i . Such entities are treated as hard-core bosons with spin- $\frac{1}{2}$ commutation relations, $[\rho_i^+, \rho_i^-]_- = 2\rho_i^z$ and $[\rho_i^+, \rho_j^-]_+ = \delta_{ij}$. $a_i^{(+)}$ denote annihilation (creation) operators of the excitations of local lattice displacements, M is some atomic mass characterizing the effective sites, and ω_0 is the frequency of the dynamical local lattice deformations. $c_i^{(+)}$ are the annihilation (creation) operators for the itinerant electrons with spin σ , $n_{i\sigma} = c_{i\sigma}^+ c_{i\sigma}^-$ being the related number operator. The bare nearest-neighbor hopping integral for such electrons is given by t , corresponding to a bandwidth $2D = 2zt$ where z denotes the lattice coordination number. The other parameters of the model are the bare bosonic energy level Δ_B , the coupling α of the local electron pairs to the surrounding lattice deformations and the bare exchange coupling v between the bosons and the pairs of itinerant electrons. The chemical potential μ , being common to electrons and bosons, guarantees the overall charge conservation. This model has been studied extensively in the limit of zero coupling ($\alpha = 0$) to the lattice, particularly in connection with the pseudogap effect in the HTSC induced by the resonant pairing of the electrons. The basic idea behind it is that the closeness of a weakly bound two-electron state to the energy level of two itinerant electrons induces resonant pairing with substantial lifetime in the electronic subsystem. This is an effect which is analogous to the atom pairing induced by Feshbach resonance in trapped ultracold gases, studied in connection with their condensed states¹⁴. The onset temperature T^* for electron pairing is determined by the strong drop-off with decreasing temperature of the on-site correlation function $\langle \rho_i^+ c_{i\downarrow}^- c_{i\uparrow}^+ \rangle$ when passing through $T = T^*$ ¹⁵. The change in this correlation function is independent on any onset of long-range phase coherence and is described by mere amplitude fluctuations. Using a variational wave function of the form

$$\prod_i [u(i) + v(i)\rho_i^+] |0\rangle \sum_k [u_k + v_k c_{k\uparrow}^+ c_{-k\downarrow}^+] |0\rangle, \quad (2)$$

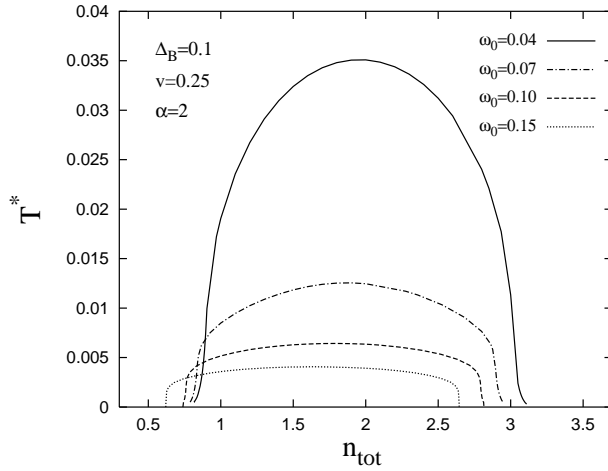


FIG. 1: T^* as a function of n_{tot} for a variety of different local phonon frequencies ω_0

we see that the exchange coupling term of the Hamiltonian (1) becomes

$$v\rho x + vx \sum_i [\rho_i^+ + \rho_i^-] + \frac{v\rho}{2} \sum_i [c_{-k\downarrow} c_{k\uparrow} + c_{k\uparrow}^+ c_{-k\downarrow}^+] \quad (3)$$

with

$$x = \frac{1}{N} \sum_i \langle c_{i\uparrow}^+ c_{i\downarrow}^+ \rangle, \quad \rho = \frac{1}{N} \sum_i \langle \rho_i^+ + \rho_i^- \rangle \quad (4)$$

denoting the amplitudes of the order parameters of the electron and boson subsystems. Thus, any inter-site phase fluctuations are explicitly suppressed in such a mean-field approximation. It hence guarantees that the resulting transition is exclusively due to amplitude fluctuations and thereby lends itself to describe the onset of pairing without any simultaneous onset of phase coherence. That this approach for determining T^* is qualitatively and, to a large extent, also quantitatively correct, was checked with a comparative study based on exact diagonalization procedures¹⁵ and self-consistent perturbative approaches¹⁶. The rapid but smooth drop-off of the local correlation function $\langle \rho_i^+ c_{i\downarrow} c_{i\uparrow} \rangle$ at T^* in those studies is then apparent as a sharp drop-off to zero of the same function at a mean-field critical temperature T_{MFA}^* . Generally T_{MFA}^* is found to lie slightly below T^* determined in more elaborate treatments, but shows the same dependence on the charge carrier concentration. This justifies the use of an analogous mean-field type procedure for the generalized boson-fermion model presented above in Eqs.(1-4), in order to extract a T^* when the coupling of the lattice vibrations to the charge carriers is turned on.

A detailed account of this mean-field analysis has been given in ref. [11] where we associated our results to a superconducting phase, assumed to be controlled exclusively by amplitude fluctuations. The true superconducting phase for this model is however known to be controlled by phase fluctuations¹⁶, while its mean-field phase

describes the pseudogap regime in an approximate form. For the purpose of the present study we shall adopt such a mean field analysis for which we shall here merely sketch the procedure.

Since the mean-field decoupling leading to Eq. (3) separates the fermionic part from the bosonic bound electron pairs, we can write the eigenstates of this Hamiltonian as a direct product of the two separate Hilbert spaces associated with fermions and bosons in the form

$$|\Psi^F\rangle \otimes \prod_i |\ell\rangle_i^B, \quad (5)$$

with

$$|\Psi^F\rangle = \prod_k [u_k + v_k c_{k\uparrow}^+ c_{-k\downarrow}^+] |0\rangle \quad (6)$$

$$|\ell\rangle_i^B = \sum_n [u_{ln}(i) + v_{ln}(i) \rho_i^+] |0\rangle_i |n\rangle_i. \quad (7)$$

Here $|0\rangle$ and $|0\rangle$ are the vacuum states for fermions and bosons, respectively, and $|n\rangle$ is the n -th excited harmonic oscillator state. It should be noted that phonons are only connected to bosons and thus the contribution (7) is the only one requiring numerical diagonalization. Denoting the eigenvalues of the two mean-field states (6) and (7) by $\tilde{\varepsilon}_{\mathbf{k}}(\rho) = \pm \sqrt{(\varepsilon_{\mathbf{k}} - \mu)^2 + (v\rho)^2/4}$ (which differs from the bare electron dispersion $\varepsilon_{\mathbf{k}}$ by showing a gap of size $v\rho$) and $E_l(x)$, we have the following selfconsistent equations for the order parameters and the concentration of electrons and local pairs

$$x = -\frac{v\rho}{4N} \sum_{\mathbf{k}} \frac{1}{\tilde{\varepsilon}_{\mathbf{k}}(\rho)} \tanh \frac{\beta \tilde{\varepsilon}_{\mathbf{k}}(\rho)}{2}, \quad (8)$$

$$\rho = \frac{1}{Z} \sum_{ln} u_{ln} v_{ln} \exp [-\beta E_l(x)], \quad (9)$$

$$n_{tot} = \frac{1}{4} \rho^2 + 2 - \frac{1}{N} \sum_{\mathbf{k}} \left(\frac{\varepsilon_{\mathbf{k}}}{\tilde{\varepsilon}_{\mathbf{k}}(\rho)} \tanh \frac{\beta \tilde{\varepsilon}_{\mathbf{k}}(\rho)}{2} \right) + \frac{1}{Z} \sum_{ln} [(u_{ln})^2 - (v_{ln})^2] \exp [-\beta E_l(x)]. \quad (10)$$

Here $Z = \sum_l \exp [-\beta E_l(x)]$ denotes the partition function corresponding to the bosonic part of the mean-field Hamiltonian, given by

$$H_B = (\Delta_B - 2\mu) \sum_i \left(\rho_i^z + \frac{1}{2} \right) + vx \sum_i [\rho_i^+ + \rho_i^-] - \hbar \omega_0 \alpha \sum_i \left(\rho_i^z + \frac{1}{2} \right) (a_i + a_i^+) + \hbar \omega_0 \sum_i a_i^+ a_i. \quad (11)$$

The onset temperature T^* for electron pairing is then determined by solving the above set of equations in the limit $x \rightarrow 0, \rho \rightarrow 0$.

We assume an electronic band extending from $-D$ to D and choose a set of parameters $\alpha = 2, \Delta_B = 0.1, v = 0.25$, with the phonon frequency ω_0 varying in the range

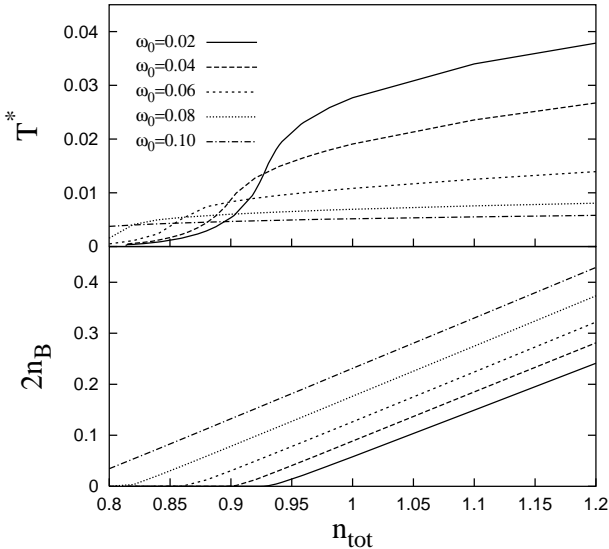


FIG. 2: T^* (top panel) and $2n_B$ (bottom panel) as a function of n_{tot} for a variety of different local phonon frequencies ω_0

[0.01, 0.1], such as to cover the intermediate polaronic situation (all energies are in units of the half-bandwidth D). This choice, leading to values of T^* of the order of a few hundred degrees K ($T^* \simeq 10^2 D$), ensures that upon changing the total number of charge carriers n_{tot} , one covers the regime of electron concentration close to half filling, with the possibility of having a drastic decrease of T^* with small variations of n_{tot} .

We present in Fig. 1 the variation of T^* as a function of n_{tot} for several values of the local phonon frequency ω_0 . As ω_0 is increased, we observe the following two main effects: (i) a shift of the whole curve $T^*(n_{tot})$ to lower values of n_{tot} , and (ii) an overall diminution of the value of T^* . The first effect is due to a shift $\delta\Delta_B \simeq \Delta_B - \varepsilon_{BP}$ of the bosonic energy level associated with the bipolaron binding energy $\varepsilon_{BP} = \alpha^2 \hbar \omega_0$. The second effect is due to the decrease of the effective exchange coupling term, determined by the reduced overlap of the lattice deformations corresponding to the presence of bipolarons and free electrons, respectively, on a given site. In the extreme strong coupling limit $\alpha^2 \hbar \omega_0 \geq D$ this renormalization would correspond to $v \rightarrow v e^{-\alpha^2}$, but remains of reasonable size and is frequency dependent in the intermediate coupling case. In conclusion, reducing n_{tot} with doping or increasing ω_0 upon increasing the isotope mass, leads to qualitatively similar results in the shift of T^* as already pointed out by some experimental observations⁸.

III. THE RESONATING PAIRING ISOTOPE EFFECT

We shall focus here on a regime of doping (n_{tot}) and local phonon frequency (ω_0) where T^* shows a rapid drop-off upon decreasing the total number of charge carriers

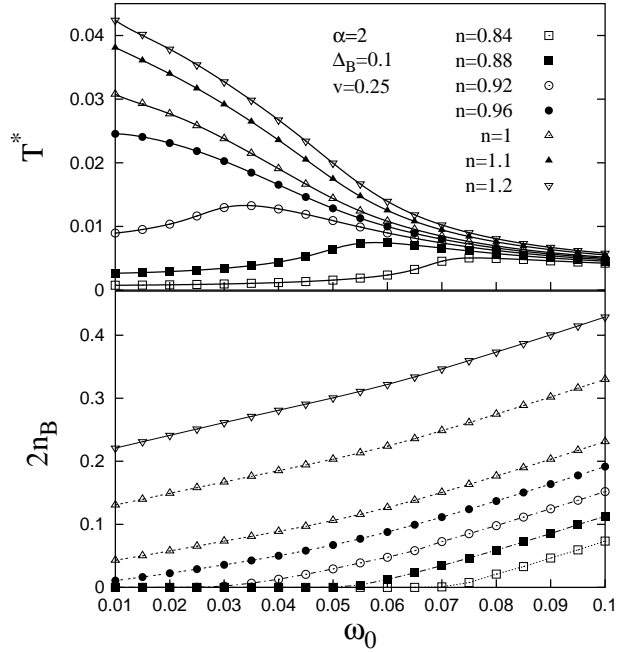


FIG. 3: T^* (top panel) and $2n_B$ (bottom panel) as a function of the local phonon frequency ω_0 and for a variety of different n_{tot}

n_{tot} over a relatively small range of values, i.e., [0.8, 1.2]. This choice is made in an attempt to account for the anomalous behavior of the isotope coefficient α^* observed in the HTSC, which in the underdoped to optimal doping regime shows unusual and negative values. In order to show the evolution of this isotope effect upon going from the underdoped to the overdoped case (the latter assumed to be more BCS-like), we examine how α^* changes with the particle density. For doping rates n_{tot} such that n_B is finite but small we have resonant pairing of the electron pairs due to their exchange with localized bipolarons. On the contrary, if n_B is exponentially small these exchange processes are purely virtual processes. We then have a situation where two-particle pairing can no longer be realized except via a true many-body effect describing Cooper pairing. The corresponding T^* then signals simultaneous pairing and onset of superconductivity together with an isotope exponent which is positive.

The behavior of T^* as a function of n_{tot} and ω_0 is controlled by two competing effects:

(i) T^* increases with increasing n_{tot} when n_B varies between 0 and 0.5.

(ii) T^* , for a fixed n_B , decreases with increasing ω_0 because of the polaron induced reduction of the exchange coupling v . But since an increase of ω_0 not only reduces the effective exchange coupling but also leads to an increased bipolaron level shift which in turn increases n_B for a fixed n_{tot} , T^* is in general a non-monotonic function of ω_0 .

We present in Fig. 2 the variation of T^* and n_B as a function of n_{tot} in the above mentioned regime of pa-

rameters. We notice the onset of a rapid rise of T^* with increasing n_{tot} controlled by an equally rapid rise of n_B . Upon further increasing n_{tot} , T^* starts to saturate, an effect due to the hard-core nature of the localized bipolarons which becomes important when n_B approaches 0.5.

The variation of T^* and n_B with ω_0 for a set of different n_{tot} is illustrated in Fig. 3. For sufficiently large values of n_{tot} , such that n_B is finite but still lower than 0.5, we find a monotonically decreasing function with increasing ω_0 , controlled by the polaron induced reduction of the effective exchange coupling v . As n_{tot} decreases, leading to a vanishing concentration of bipolarons, the behavior of T^* changes qualitatively. For low values of ω_0 , the polaron induced reduction of the effective exchange coupling is negligible and T^* now increases with increasing ω_0 because it is controlled by the increase of n_B . With increasing ω_0 , the effect of the polaron induced reduction of the exchange coupling becomes competitive with the increase of n_B such that the initial increase of T^* with increasing ω_0 changes into a decreasing behavior.

Provided we are in the regime of resonant pairing, with n_B small but finite and T^* monotonically decreasing with decreasing n_{tot} , Fig. 3 tells us the following. T^* is shifted upwards by the decrease of the phonon frequency associated with the increase of the isotope mass (as realized, for instance, replacing ^{16}O by ^{18}O), and this effect becomes less and less pronounced as doping increases (n_{tot} decreases). Moreover, if for a given doping level the isotope substitution is made for heavier elements, such as ^{63}Cu replaced by ^{65}Cu , the increase of the corresponding T^* is getting smaller and smaller, as one can deduce from the behavior of T^* at low ω_0 . These features are in qualitative agreement with experimental findings in LaSrHoCuO_4 compounds^{9,10}.

In order to determine the isotope coefficient, which it-self will depend on ω_0 and n_{tot} , we have first interpolated the calculated values of T^* by a ratio of polynomials, and then derived α^* from the relation

$$\alpha^* = 0.5 \ln \left(\frac{T^*(i)}{T^*(i+1)} / \frac{\omega_0(i)}{\omega_0(i+1)} \right) \quad (12)$$

where $\omega_0(i)$ and $\omega_0(i+1)$ represent two very close values of the phonon frequency. We present in Fig. 4 the variation of the isotope exponent as a function of the phonon frequency ω_0 for a set of different values of n_{tot} and in Fig. 5 the variation of the isotope exponent as a function of n_{tot} for a selected set of phonon frequencies ω_0 .

We notice two distinct regimes which characterize α^* :

(i) a regime where α^* is negative and depends strongly on ω_0 but shows a relative independence on the concentration n_{tot} . This happens when the corresponding n_B is big enough to sustain the mechanism of resonant pairing.

(ii) a regime of positive values of α^* which occurs when n_B drops to zero as a consequence of the decrease of n_{tot} or, alternatively, of ω_0 (see the bottom panel of Fig. 2). In this case, which corresponds to the system being more BCS-like, electron pairing arises from virtual excitations

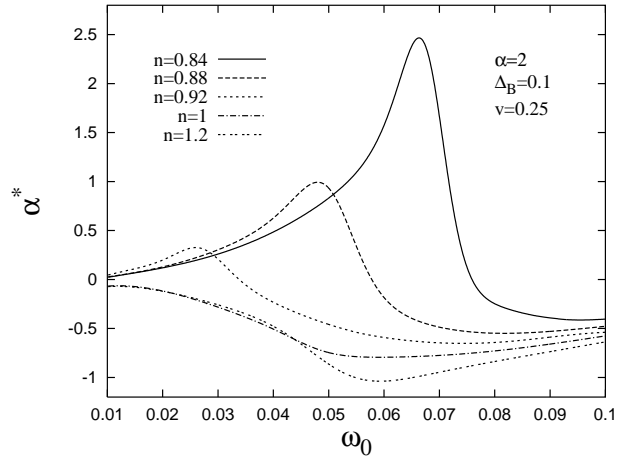


FIG. 4: α^* as a function of the local phonon frequency ω_0 and for a variety of different n_{tot}

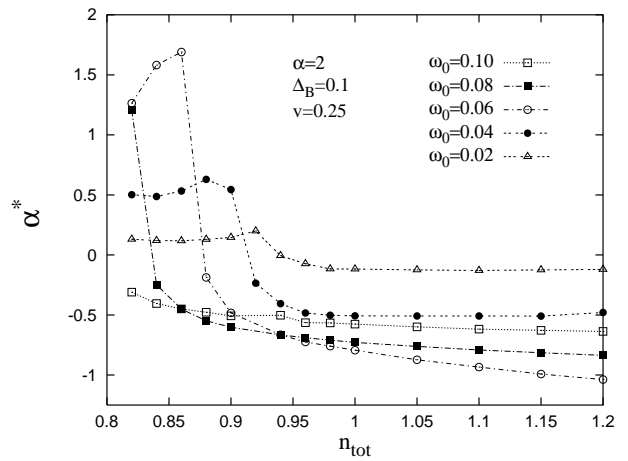


FIG. 5: α^* as a function of n_{tot} and for a variety of different local phonon frequencies ω_0 .

of the electrons into bipolaronic localized states above the Fermi level and the onset of pairing at T^* coincides with the onset of superconductivity.

These two regimes are clearly visible in the variation of the gap ratio $2\Delta(0)/(k_B T^*)$, where $2\Delta(0) = v\rho(0)$ is the zero temperature gap in the Fermionic excitation spectrum $\tilde{\varepsilon}_k$. This ratio, which is shown in Fig. 6 as a function of n_{tot} for several ω_0 , is a slowly-varying function of the concentration when the system is well inside the resonant pairing regime ($1.2 < n_{tot} < 2.8$ for our choice of ω_0 values) but strongly depends on the local phonon frequency ω_0 . For values of n_{tot} such that n_B becomes exponentially small (depending on ω_0 this happens below $n_{tot} = 0.9$, see bottom panel in Fig. 2), the gap ratio approaches the BCS value 3.52.

Going back to the behavior of the isotope coefficient at low n_{tot} , we stress that even in this BCS-like regime α^* shows a frequency dependence related to the pairing mechanism, which in the case studied here of strong electron-phonon interaction is different from the standard

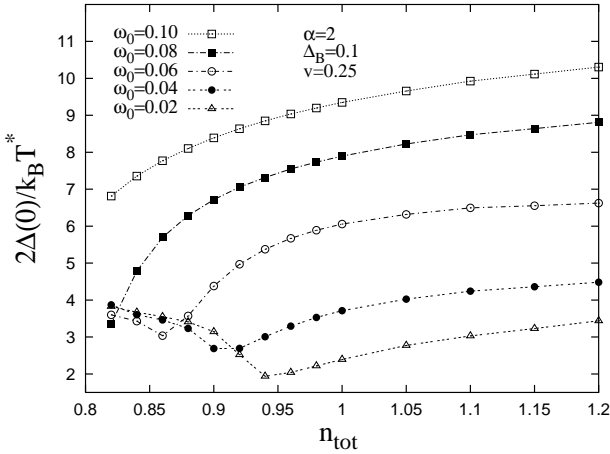


FIG. 6: $2\Delta(0)/(k_B T^*)$ as a function of n_{tot} and for a variety of different local phonon frequencies ω_0 .

weak-coupling BCS one. In our model, pairing among the electrons is induced via virtual excitations of electron pairs into a localized bipolaron state and an effective BCS-like Hamiltonian for this situation can be derived along the following two steps:

- the boson-phonon coupling is incorporated into an effective boson-fermion exchange interaction $\tilde{v} = v \exp(-\alpha^2/2)$ via a Lang-Firsov approximation;
- the boson-fermion coupling term is subsequently eliminated to linear order via the usual unitary transformation

$$\tilde{H} = e^S H e^{-S} \quad (13)$$

$$S = \sum_{i,k} f(k) [\rho_i^+ c_{-k\downarrow} c_{k\uparrow} - \text{H.c.}] \quad (14)$$

$$f(k) = \frac{\tilde{v}}{2\varepsilon_k - \Delta_B + \varepsilon_{BP}} \quad (15)$$

which in the end results in an effective BCS-like Hamiltonian of the form

$$\begin{aligned} \tilde{H} = & \sum_{k,\sigma} (\varepsilon_k - \mu) c_{k\sigma}^+ c_{k\sigma} \\ & + \frac{\tilde{v}^2}{2} \sum_{k,k'} [f(k) + f(k')] c_{k\uparrow}^+ c_{-k\downarrow}^+ c_{-k'\downarrow} c_{k'\uparrow}. \end{aligned} \quad (16)$$

In the standard weak-coupling effective BCS Hamiltonian, the interaction term is restricted to the summation over k -vectors within a small energy range around the Fermi surface of width given by the Debye temperature Θ_D . This gives rise to an effective interaction of the order of Θ_D from which a frequency independent isotope shift follows, with an isotope exponent equal to 0.5.

The effective Hamiltonian for our scenario, eq. 16, shows on the contrary no such a cutoff in energy and extends the pairing of electrons over all k vectors below the Fermi vector, albeit with different weight. Moreover, because of the presence of the bipolaronic energy in the

denominator of eq. 15, the effective interaction is attractive in this regime of low bipolaron concentration, since $2\varepsilon_{kF} < \Delta_B - \varepsilon_{BP}$, and grows in magnitude as ω_0 increases. This is the reason why we obtain a frequency dependent isotope shift even in this BCS-like regime with a T^* which increases as ω_0 increases.

IV. CONCLUSIONS

Experimentally, there are strong indications that in the HTSC the isotope coefficient associated with the temperature T^* at which the pseudogap in the underdoped regime opens up, is negative. Its precise numerical value depends on the type of material, the doping regime, the type of isotope substitution ($^{16}\text{O} \leftrightarrow ^{18}\text{O}$, $^{63}\text{Cu} \leftrightarrow ^{65}\text{Cu}$) as well as on the different time scales of the various experiments. Presently, there exist to our knowledge no systematic experimental studies which would permit to test a particular theoretical approach on this issue in detail. The study presented here was designed to incite experimental work to explore specifically the doping dependence of the resonant pairing isotope effect, given the characteristic strong doping dependence of T^* in the HTSC. If we assume that this feature is related to a two-component scenario with localized charge carriers (such as bipolarons) and itinerant electrons, with the sharp drop of T^* being essentially governed by a doping dependent change of the bipolaron thermal population, the isotope effect on T^* should exhibit a corresponding concentration dependence. In agreement with experiments, we find indeed a negative value for the isotope exponent, as long as pairing is assured by a resonant scattering between the localized bipolarons and the free electrons. However, as soon as upon doping we enter a regime where the bipolaron level moves above the Fermi energy, pairing is only possible via a collective effect such as Cooper pairing and the isotope exponent switches sign and becomes positive. With respect to the HTSC, this could happen when going from the underdoped into the overdoped regime. Considering, however, that the lattice mediated coupling between electrons in the present scenario is different from the standard phonon-induced Cooper pairing, we obtain a behavior for the isotope exponent which deviates from that of standard low temperature BCS superconductors. Although it converges to a value independent on doping as n_{tot} is reduced such that n_B becomes exponentially small (see the curves at low ω_0 in Fig. 5), it nevertheless continues to sensitively depend on the characteristic local phonon frequency ω_0 .

The present mean-field type study is expected to qualitatively correctly describe the doping dependence of α^* in the resonant pairing regime where T^* is controlled by amplitude fluctuations. This mean-field scheme treats the local dynamical atomic displacements as correlated to the local density fluctuations between the electrons and the bipolarons, which in our model, are responsible for the opening of the pseudogap. It is this mecha-

nism which is at the origin of the blockage of the crystal field excitations which below T^* couple to the free charge carriers, as observed experimentally in neutron spectroscopic measurements testing the transitions between different crystal field levels^{8,9}. A more quantitative analysis than the mean-field procedure presented here would be required in order to account for the dynamical nature of the onset of pairing, as seen in experiments with different time scales¹⁷ which lead to different absolute values of T^* but to qualitatively similar doping dependence of T^* . Such a highly non-trivial undertaking is however beyond the scope and purpose of the present work.

We want to stress that the scenario described here is based on a mechanism originating from *purely local* dynamical lattice instabilities for which experimental evidence has been accumulating over the past few years. Inelastic neutron scattering measurements have shown strong compositional dependence of certain optical (half-

breathing zone-edge) phonon modes, which were linked to spatial local charge inhomogeneities¹⁸ of small clusters and suggest that the lattice is strongly involved in the charge dynamics. EXAFS studies¹⁹ tracked such local charge inhomogeneities in form of a significant deviation from a systematic Pauling-type shift of the planar Cu–O bonds, when the bonding mechanism changes from ionic to more covalent nature as doping is increased. Similarly, very recent tunneling spectroscopic studies²⁰ indicate the existence of local charge density modulations involving local spatial correlations of four CuO₂ unit cells, referred to as "squared checkerboard" structures. All these findings go in the direction of *local* charge inhomogeneities as well as *local* dynamical lattice deformations, against earlier propositions of long-range stripe order, on the basis of which the pseudogap isotope effect was theoretically investigated previously²¹.

¹ J. Orenstein, G. A. Thomas, D. H. Rappine, C. G. Bethea, B. F. Levine, B. Batlogg, R. J. Cava, D. W. Johnson, Jr., and E. A. Rietman, Phys. Rev. B **36**, 8892 (1987).

² S. Etemad, D. E. Aspnes, M. K. Kelly, R. Thompson, J. M. Tarascon, and G. W. Hull, Phys. Rev. B **37**, 3396 (1988).

³ X. X. Bi and P. C. Eklund, Phys. Rev. Lett. **70**, 2625 (1993).

⁴ R. J. McQueeney, J. L. Sarrao, P. G. Pagliuso, P. W. Stephens, and R. Osborn, Phys. Rev. Lett. **87**, 077001 (2001).

⁵ A. Lanzara, P. V. Bogdanov, X. J. Zhou, S. A. Kellar, D. L. Feng, E. D. Lu, T. Yoshida, H. Eisaki, A. Fujimori, K. Kishio, J.-I. Shimoyama, T. Noda, S. Uchida, Z. Hussain, and Z.-X. Shen, Nature (London) **412**, 510 (2001).

⁶ L. Pintschovius, W. Reichardt, M. Kläser, T. Wolf, and H. v. Löhneysen, Phys. Rev. Lett. **89**, 037001 (2002).

⁷ A. Lanzara, Guo-meng Zhao, N. L. Saini, A. Bianconi, K. Conder, H. Keller, and K. A. Müller, J. Phys.: Cond. Matt. **11**, L541 (1999).

⁸ D. Rubio Temprano, J. Mesot, S. Janssen, A. Furrer, K. Conder, and H. Mutka, Phys. Rev. Lett. **84**, 1990 (2000).

⁹ D. Rubio Temprano, K. Conder, A. Furrer, H. Mutka, V. Trounov, and K. A. Müller, Phys. Rev. B **66**, 184506 (2002).

¹⁰ A. Furrer, K. Conder, P. Häfliger, and A. Podlesnyak, Physica C **408**, 773 (2004).

¹¹ J. Ranninger and A. Romano, Phys. Rev. B **66**, 094508 (2002).

¹² J. Ranninger and A. Romano, Phys. Rev. Lett. **80**, 5643 (1998).

¹³ E. V. L. de Mello and J. Ranninger, Phys. Rev. B **55**, 14872 (1997).

¹⁴ E. Timmermans, P. Tommasini, M. Hussein, and A. Kerman, Phys. Rep. **315**, 199 (1999).

¹⁵ M. Cuoco, C. Noce, J. Ranninger, and A. Romano, Phys. Rev. B **67**, 224504 (2003).

¹⁶ J. Ranninger and L. Tripodi, Phys. Rev. B **67**, 174521 (2003).

¹⁷ Guo-meng Zhao, H. Keller, and K. Conder, J. Phys.: Cond. Matt. **13**, R569 (2001).

¹⁸ J.-H. Chung, T. Egami, R.J. McQueeney, M. Yethiraj, M. Arai, T. Yokoo, Y. Petrov, H.A. Mook, Y. Endoh, S. Tajima, C. Frost, and F. Dogan, Phys. Rev. B **67**, 014517 (2003).

¹⁹ J. Roehler, cond-mat/0407654 (to be published in Int. J. Mod. Phys. B).

²⁰ T. Hanaguri, C. Lupien, Y. Kohsaka, D.H. Lee, M. Azuma, M. Takano, H. Takagi, and J.C. Davis, Nature **430**, 1001 (2004).

²¹ S. Andergassen, S. Caprara, C. Di Castro, and M. Grilli, Phys. Rev. Lett. **87**, 56401 (2001).